Available online at www.sciencedirect.com
ScienceDirect
International Journal of Heat and Mass Transfer 51 (2008) 3556–3570
International Journal of HEAT and MASS TRANSFER
www.elsevier.com/locate/ijhmt

Transient heat conduction in a medium with two circular cavities: Semi-analytical solution

Elizaveta Gordeliy *, Steven L. Crouch, Sofia G. Mogilevskaya

Department of Civil Engineering, University of Minnesota, Minneapolis, MN 55455, USA

Received 2 March 2007; received in revised form 15 October 2007
Available online 14 January 2008

Abstract

This paper considers a transient heat conduction problem for an infinite medium with two non-overlapping circular cavities. Suddenly applied, steady Dirichlet type boundary conditions are assumed. The approach is based on superposition and the use of the general solution to the problem of a single cavity. Application of the Laplace transform results in a semi-analytical solution for the temperature in the form of a truncated Fourier series. The large-time asymptotic formulae for the solution are obtained by using the analytical solution in the Laplace domain. The method can be extended to problems with multiple cavities and inhomogeneities.

Keywords: Transient heat conduction; Laplace transform; Modified Helmholtz equation; Fourier series; Addition theorem; Asymptotic series

1. Introduction

This paper presents a semi-analytical solution for a transient heat conduction problem for an infinite medium containing two circular cavities. This problem occurs in several engineering applications, for example, heat exchange between the earth and buried pipes [1], cooling of tunnels [2], and heat exchange between blood tissue and embedded blood vessels [3]. The problem is also of interest for modeling time-dependent effects due to diffusion processes, such as unsteady fluid flow [4,5].

As in many other applications, the use of analytical solutions in transient heat conduction problems is very beneficial. Such solutions can be used to study possible singularities, to obtain accurate solution gradients (e.g. heat fluxes), as well as the asymptotic approximations for the solutions for small and large values of time. In addition, knowledge of analytical solutions can provide benchmark results to test newly developed numerical methods.

The method of solution presented here for a problem of two circular cavities is based on the use of the analytical solution to a corresponding problem of a single cavity and superposition. The single cavity problem has been extensively studied and various particular solutions are available in the literature (e.g. [6]). Analytical and semi-analytical solutions for the case of multiple cavities are available only for the steady-state case (e.g. [3,6]).

Transient problems with cavities can be solved by general purpose numerical methods such as finite element, finite difference, and boundary element methods combined with time-marching schemes. For large-time computations these approaches can be computationally intensive due to time-marching and large numbers of degrees of freedom. To efficiently treat the time convolution involved in the problem several fast numerical techniques have been recently developed (see e.g. [7–9] and references therein).

A number of numerical methods based on the use of the Laplace transform (or Fourier transform) have also been designed to solve transient problems. In such methods the original transient problem is transformed to a corresponding non-transient problem in the Laplace domain (or frequency domain), which is easier to solve. After the

* Corresponding author. Tel.: +1 612 626 8768; fax: +1 612 626 7750.
E-mail address: gord0232@umn.edu (E. Gordeliy).

0017-9310/$ - see front matter © 2007 Elsevier Ltd. All rights reserved.
doi:10.1016/j.ijheatmasstransfer.2007.10.021

Nomenclature

$\binom{m}{n}$ binomial coefficient, $\binom{m}{n} = \frac{m!}{n!(m-n)!}$
a_k intermediate variable, $a_k = r_k/R_k$
$\mathbf{a}^k(x,s)$ (N_k+1)-dimensional vector, Eq. (23)
$\mathbf{a}^k_{pm}(x)$ vector coefficients of the asymptotic expansion of $\mathbf{a}^k(x,s)$, Eq. (31)
$A_{pm}(x)$ coefficients of the asymptotic expansion of $\widehat{T}(x,s)$, Eq. (29)
$A^{kl}_n(s)$, $B^{kl}_n(s)$ Fourier coefficients of the boundary value $\widehat{T}_l(x,s)|_{L_k}$ $(k \neq l)$, Eq. (13)
$\mathbf{A}^{kl}(s)$ (N_k+1)-dimensional vector of Fourier coefficients $A^{kl}_n(s)$, Eq. (14)
$B^{p,i}_{m-i}$ intermediate coefficients, Appendix D
$\mathbf{B}^{kl}(s)$ N_k-dimensional vector of Fourier coefficients $B^{kl}_n(s)$, Eq. (14)
$\mathbf{b}^k(x,s)$ N_k-dimensional vector, Eq. (23)
$\mathbf{b}^k_{pm}(x)$ vector coefficients of the asymptotic expansion of $\mathbf{b}^k(x,s)$, Eq. (32)
c^k_n, d^k_n Fourier coefficients of the function $\Phi_k(\varphi_k)$, Eq. (5)
$\mathbf{c}^k$ (N_k+1)-dimensional vector of Fourier coefficients c^k_n, Eq. (14)
$\mathbf{d}^k$ N_k-dimensional vector of Fourier coefficients d^k_n, Eq. (14)
$\mathbf{F}^{kl}(s)$ $(N_k+1)\times(N_l+1)$-dimensional matrix $(k \neq l)$, Eq. (15)
$\mathbf{F}^{kl}_{pm}$ matrix coefficients of the asymptotic expansion of $\mathbf{F}^{kl}(s)$, Eq. (64)
$f(u)$ integrand matrix-function, Section 6.2
$\mathbf{G}^{kl}(s)$ $N_k \times N_l$-dimensional matrix $(k \neq l)$, Eq. (15)
$\mathbf{G}^{kl}_{pm}$ matrix coefficients of the asymptotic expansion of $\mathbf{G}^{kl}(s)$, Eq. (65)
H_k steady-state flux, Eq. (28)
$\mathbf{I}_N$ $N \times N$-dimensional identity matrix
$I_n(\cdot)$, $K_n(\cdot)$ modified Bessel functions [21]
k, l number of the cavity, $k = 1,2$ and $l = 1,2$
L_k boundary of the kth cavity
M number of steps in the alternating algorithm, Eqs. (51) and (52)
M_0, M_1 numbers of terms in asymptotic series (29) and (44)
$\mathbf{m}^k_{0,-1}$ $1 \times (N_k+1)$-dimensional matrix, Appendix C
N_k number of terms in the truncated Fourier series, Eq. (10)
$\mathbf{n}^k$ annihilating vector, Section 5.1
q transform variable, $q = \sqrt{s}$
R_k dimensionless ratio of the radius of the kth cavity to the distance ρ
r_k dimensionless radial polar coordinate = ratio of the distance between point x and the center of the kth cavity to the distance ρ
$\mathbf{R}^k_{npm}$ right-hand side matrices in Eq. (82)
s Laplace transform parameter
t dimensionless time, Eq. (1)
t_1 minimum specified time instant, Section 6
t_n dimensionless time, at which the solution is computed, Section 6
$T(x,t)$ dimensionless temperature, Eq. (1)
$T_s(x)$ steady-state temperature, Eqs. (26) and (27)
$\widehat{T}(x,s)$ Laplace transform of $T(x,t)$
$\widehat{T}_k(x,s)$ solution to the Laplace-transformed problem containing only the kth cavity, Eq. (9)
u integration variable, Eq. (26)
$\mathbf{U}^k(s)$ $(N_k+1)\times(N_k+1)$-dimensional matrix, Eq. (19)
$\mathbf{U}^k_{pm}$ matrix coefficients of the asymptotic expansion of $\mathbf{U}^k(s)$, Eq. (37)
$\widetilde{\mathbf{U}}^k_{pm}$ matrix coefficients of the asymptotic expansion of $[\mathbf{U}^k(s)]^{-1}$, Eq. (34)
$\mathbf{u}^k(s)$ (N_k+1)-dimensional vector, Eq. (19)
$\mathbf{u}^k_{pm}$ vector coefficients of the asymptotic expansion of $\mathbf{u}^k(s)$, Eq. (75)
$\mathbf{V}^k(s)$ $N_k \times N_k$-dimensional matrix, Eq. (20)
$\mathbf{V}^k_{pm}$ matrix coefficients of the asymptotic expansion of $\mathbf{V}^k(s)$, Eq. (38)
$\widetilde{\mathbf{V}}^k_{pm}$ matrix coefficients of the asymptotic expansion of $[\mathbf{V}^k(s)]^{-1}$, Eq. (35)
$\mathbf{v}^k(s)$ N_k-dimensional vector, Eq. (20)
$\mathbf{v}^k_{pm}$ vector coefficients of the asymptotic expansion of $\mathbf{v}^k(s)$, Eq. (76)
x point in the two-dimensional domain
x_m point in the two-dimensional domain, at which the solution is computed, Section 6
$Y^k_n(s)$, $Z^k_n(s)$ unknown Fourier coefficients, Eq. (10)
$\mathbf{Y}^k(s)$ (N_k+1)-dimensional vector of unknowns, Eq. (14)
$\mathbf{Z}^k(s)$ N_k-dimensional vector of unknowns, Eq. (14)

Greek symbols

α_k, β_k, β intermediate constants, Eq. (55)
γ Euler's constant, $\gamma = 0.5772\ldots$
δ intermediate integration limit, Eq. (50)
δ_{ij} Kronecker delta symbol
ε predefined accuracy level, Eq. (47)
$\Theta(x,\tau)$ temperature at point x at time τ
Θ_0 uniform initial temperature, $\Theta_0 = \Theta(x,0)$
κ constant thermal diffusivity
$\Lambda_{pm}(x)$ coefficients of the large-time asymptotic series, Eq. (44)
μ_k scalar factor, Appendix C
ρ distance between the centers of the cavities
τ time

Υ_n	components of the generic vectors $\boldsymbol{\Upsilon}_{N_k+1}$ and $\boldsymbol{\Upsilon}_{N_k}$, Eq. (14)
$\boldsymbol{\Upsilon}_{N_k+1}$, $\boldsymbol{\Upsilon}_{N_k}$	generic vectors, Eq. (14)
$\Phi_k(\varphi_k)$	specified boundary temperature at the boundary L_k
φ_k	polar angle in the coordinate system of the kth cavity ($-\pi < \varphi_k \leqslant \pi$), Fig. 1b
$\psi^{(n)}(x)$	polygamma function [21]

Subscripts

k, l	number of the cavity, $k = 1, 2$ and $l = 1, 2$
n, m, p	summation indices

Superscripts

k, l	number of the cavity, $k = 1, 2$ and $l = 1, 2$
T	transposition operator

solution to the transformed problem is obtained, the inverse transform needs to be performed to obtain the solution in the original time space. Most of these methods solve the non-transient transformed problem numerically (e.g. by using a finite element method (e.g. [10,11]) or a boundary element method (e.g. [12–15])) and perform numerical inversion of the Laplace (or Fourier) transform.

Another Laplace-transform-based method is presented in [5], where it was used to solve a problem of transient flow in media with circular inhomogeneities by means of the analytic element method. The analytic element method was originally suggested by Strack [16] for steady flow problems. A detailed description of the method and a list of early references can be found in the monograph [17]. Further developments and relevant references can be found in [18,19]. In this method, the solution of the problem is taken as a superposition of series of analytical solutions of the governing differential equation corresponding to each inhomogeneity. The unknown series coefficients are found using collocation and least squares techniques such that boundary conditions are satisfied along given boundaries. Applications of the analytic element method to problems with multiple circular inhomogeneities can be found in [19,20]. To solve transient flow problems, the analytic element based method presented in [5] is applied to the Laplace-transformed problem governed by the modified Helmholtz equation. A numerical inversion of the Laplace transform is performed to obtain the solution in the original time domain. A solution of the modified Helmholtz equation in media with multiple circular inhomogeneities by means of the analytic element method is also studied in [19].

Our method is also based on the use of the Laplace transform and the superposition method. For each cavity the solution is taken as a truncated Fourier–Bessel series in the local polar coordinate system of that cavity, where the series coefficients are unknown. The novelty of our approach is that, due to the use of Fourier series approximations and Graf's addition theorem for Bessel functions [21], most of the derivations involved in the mathematical basis of the algorithm can be done analytically. The application of the addition theorem allows one to analytically re-expand the basis functions corresponding to one cavity in terms of an infinite series of basis functions corresponding to the other cavity. After proper truncation of those series, both sides of the transformed boundary equation for each cavity can be expressed in terms of truncated series of basis functions related to this cavity. The unknown series coefficients can be found from a linear system of algebraic equations. The only error introduced in this process is due to the truncation of the series expansions.

Finally, inversion of the Laplace transform is performed using the complex integral inversion formula [6]. The integration along some part of the integration contour is performed analytically. The integral over the remaining part of the contour is put in a convenient closed (integral) form that allows one to study the behavior of the solution as a smooth function of time and spatial coordinates, e.g. to obtain accurate solution derivatives. The asymptotic large-time series for the solution is obtained using the asymptotic expansion of the analytical solution $\widehat{T}(x, s)$ in the Laplace domain and the analytical inversion of the Laplace transform.

As a result, our method allows us to accurately calculate the temperature and heat flux anywhere within the material, at any time. The use of asymptotic formulae further reduces the cost of computations.

The method can be extended further to treat problems involving multiple cavities and inhomogeneities, but this is outside the scope of the present discussion.

2. Mathematical formulation

Consider an infinite domain containing two non-overlapping circular cavities (Fig. 1a). We assume that the domain is initially at uniform temperature Θ_0 and that its thermal diffusivity κ is constant. We also assume that the boundary of each cavity is subjected to an instantly-applied steady temperature that can vary along the boundary. The temperature $\Theta = \Theta(x, \tau)$ at point x in the domain, at time τ, is to be determined.

We orient the domain in such a way that the centers of the cavities are located on a horizontal line. We will refer to the left cavity as the first cavity, and the other cavity as the second one. We define R_k as the dimensionless ratio of the radius of the kth cavity with the boundary L_k ($k = 1, 2$) to the distance ρ between the centers of the cavities. For each cavity k, we introduce a local polar coordinate system $(\rho r_k, \varphi_k)$ with the origin at the center of the cavity (Fig. 1b), where r_k is the dimensionless ratio of the distance between point x and the center of the kth cavity to the distance ρ, and where the polar angle φ_k ($-\pi < \varphi_k \leqslant \pi$) is

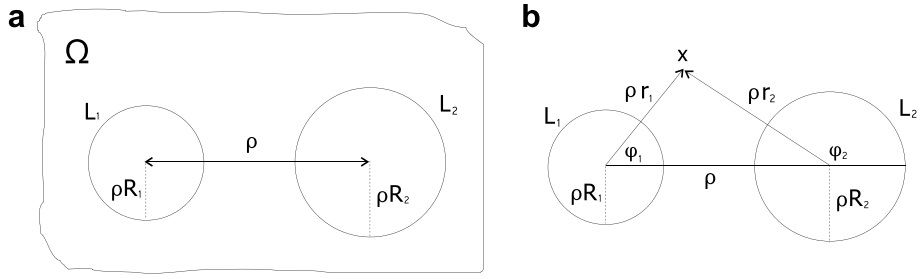

Fig. 1. Problem geometry (a) and local polar coordinate systems (b).

positive if measured counterclockwise from the line connecting the centers of the cavities as shown in Fig. 1b.

We introduce the dimensionless temperature $T = T(x,t)$ at point x at dimensionless time t as follows:

$$T(x,t) = \left[\Theta\left(x, \frac{\rho^2 t}{\kappa}\right) - \Theta_0\right] \times [\Theta]^{-1}; \quad t = \frac{\kappa\tau}{\rho^2} \tag{1}$$

where $[\Theta]$ is the unit of the temperature dimension. The governing diffusion equation [6] and the associated initial and boundary conditions are then written in dimensionless polar coordinates (r_k, φ_k) as follows:

$$\frac{\partial^2 T}{\partial r_k^2} + \frac{1}{r_k}\frac{\partial T}{\partial r_k} + \frac{1}{r_k^2}\frac{\partial^2 T}{\partial \varphi_k^2} = \frac{\partial T}{\partial t} \tag{2}$$

$$T(x,0) = 0, \quad r_k > R_k, \quad k = 1,2 \tag{3}$$

$$T(x,t)|_{L_k} = \Phi_k(\varphi_k), \quad -\pi < \varphi_k \leqslant \pi, \quad t > 0 \tag{4}$$

where $\Phi_k(\varphi_k)$ is a smooth bounded function of φ_k. We assume that $\Phi_k(\pi) = \Phi_k(-\pi)$, $\Phi_k'(\pi) = \Phi_k'(-\pi)$ and $\Phi_k''(\pi) = \Phi_k''(-\pi)$, and that $\Phi_k(\varphi_k)$ can be expanded in uniformly convergent Fourier series in φ_k as follows:

$$\Phi_k(\varphi_k) = \frac{c_0^k}{2} + \sum_{n=1}^{\infty}(c_n^k \cos n\varphi_k + d_n^k \sin n\varphi_k) \tag{5}$$

In the following, problem (2)–(4) is solved. We make the following assumptions concerning the function $T(x,t)$: (i) $T(x,t)$ is a 2π-periodic function of φ_k that has a 2π-periodic derivative with respect to φ_k, and (ii) $T(x,t)$ is finite as $r_k \to \infty$ (regularity condition).

To solve problem (2)–(4), we employ the Laplace transform, defined for a function $g(t)$ as [6]

$$\hat{g}(s) = \int_0^{\infty} \mathrm{e}^{-st} g(t)\mathrm{d}t \tag{6}$$

where $\hat{g}(s)$ is the Laplace transform of the function $g(t)$, and s is the transform parameter.

Using the properties of the Laplace transform [6], problem (2)–(4) is reformulated in the Laplace domain as follows:

$$\frac{\partial^2 \widehat{T}}{\partial r_k^2} + \frac{1}{r_k}\frac{\partial \widehat{T}}{\partial r_k} + \frac{1}{r_k^2}\frac{\partial^2 \widehat{T}}{\partial \varphi_k^2} = s\widehat{T} \tag{7}$$

$$\widehat{T}(x,s)|_{L_k} = \frac{1}{s}\left[\frac{c_0^k}{2} + \sum_{n=1}^{\infty}(c_n^k \cos n\varphi_k + d_n^k \sin n\varphi_k)\right] \tag{8}$$

where $\widehat{T}(x,s)$ is the Laplace transform of the function $T(x,t)$. Eq. (7) is the modified Helmholtz equation in polar coordinates (r_k, φ_k). This equation combines governing differential equation (2) and zero initial condition (3). In the following, we solve Eq. (7) subject to boundary conditions (8). We assume that $\widehat{T}(x,s)$ is a 2π-periodic function of φ_k that has a 2π-periodic derivative with respect to φ_k and is finite as $r_k \to \infty$ (regularity condition). As soon as the function $\widehat{T}(x,s)$ is determined, the solution $T(x,t)$ is obtained using the analytical inversion of the Laplace transform.

3. Solution in the Laplace domain

Solution $\widehat{T}(x,s)$ to Eq. (7) is sought in the form

$$\widehat{T}(x,s) = \widehat{T}_1(x,s) + \widehat{T}_2(x,s) \tag{9}$$

where $\widehat{T}_k(x,s)$ is the solution to the problem containing only the kth cavity $(k = 1,2)$ with an unknown value $\widehat{T}_k(x,s)|_{L_k}$ at the boundary L_k. The unknown value $\widehat{T}_k(x,s)|_{L_k}$ should be chosen such that $\widehat{T}(x,s)$ satisfies the boundary conditions (8).

The unknown value $\widehat{T}_k(x,s)|_{L_k}$ may be approximated by the following truncated Fourier series:

$$\widehat{T}_k(x,s)|_{L_k} = \frac{Y_0^k(s)}{2} + \sum_{n=1}^{N_k}(Y_n^k(s)\cos n\varphi_k + Z_n^k(s)\sin n\varphi_k) \tag{10}$$

where the coefficients $Y_n^k(s)$, $Z_n^k(s)$ are unknown functions of s. The number of terms N_k in the truncated series is arbitrary and may be different for each cavity. Based on the general solution of modified Helmholtz equation (7) in an infinite medium with a single cavity (for example, see [5]), the solution $\widehat{T}_k(x,s)$, finite as $r_k \to \infty$, is then written as

$$\widehat{T}_k(x,s) = \frac{Y_0^k(s)}{2}\frac{K_0(r_k q)}{K_0(R_k q)} + \sum_{n=1}^{N_k}\frac{K_n(r_k q)}{K_n(R_k q)}(Y_n^k(s)\cos n\varphi_k + Z_n^k(s)\sin n\varphi_k) \tag{11}$$

where $q = \sqrt{s}$, and $K_n(\cdot)$ is the modified Bessel function [21].

The boundary conditions (8) are rewritten in terms of truncated Fourier series as $(k, l = 1,2$ and $k \neq l)$

$$\widehat{T}_k(x,s)|_{L_k} + \widehat{T}_l(x,s)|_{L_k} = \frac{1}{s}\left[\frac{c_0^k}{2} + \sum_{n=1}^{N_k}(c_n^k \cos n\varphi_k + d_n^k \sin n\varphi_k)\right] \quad (12)$$

where $\widehat{T}_l(x,s)|_{L_k}$ is the value of the transformed temperature $\widehat{T}_l(x,s)$ along the boundary L_k. The unknown coefficients $Y_n^k(s)$ and $Z_n^k(s)$ should be chosen such that boundary conditions (12) are satisfied.

The value $\widehat{T}_l(x,s)|_{L_k}$ of the function $\widehat{T}_l(x,s)$ along the boundary L_k $(k \neq l)$ can be re-expanded in a truncated Fourier series in the polar coordinate system of the kth cavity by using Graf's addition theorem for Bessel functions [21], as follows:

$$\widehat{T}_l(x,s)|_{L_k} = \frac{A_0^{kl}(s)}{2} + \sum_{n=1}^{N_k}(A_n^{kl}(s)\cos n\varphi_k + B_n^{kl}(s)\sin n\varphi_k) \quad (13)$$

For convenience, we introduce (N_k+1)-dimensional vectors of Fourier coefficients $\mathbf{Y}^k(s)$, $\mathbf{A}^{kl}(s)$ and N_k-dimensional vectors of Fourier coefficients $\mathbf{Z}^k(s)$, $\mathbf{B}^{kl}(s)$ in the following template form:

$$[\boldsymbol{\Upsilon}_{N_k+1}]^{\mathrm{T}} = \left(\frac{\Upsilon_0}{2}, \Upsilon_1, \ldots, \Upsilon_{N_k}\right); \quad [\boldsymbol{\Upsilon}_{N_k}]^{\mathrm{T}} = (\Upsilon_1, \ldots, \Upsilon_{N_k}) \quad (14)$$

where the superscript T denotes the transposition operator[1], the generic (N_k+1)-dimensional vector $\boldsymbol{\Upsilon}_{N_k+1}$ denotes vector $\mathbf{Y}^k(s)$ or $\mathbf{A}^{kl}(s)$ with the coefficients $\Upsilon_n = Y_n^k(s)$ or $\Upsilon_n = A_n^{kl}(s)$ $(n = 0, \ldots, N_k)$ respectively, and the generic N_k-dimensional vector $\boldsymbol{\Upsilon}_{N_k}$ denotes vector $\mathbf{Z}^k(s)$ or $\mathbf{B}^{kl}(s)$ with the coefficients $\Upsilon_n = Z_n^k(s)$ or $\Upsilon_n = B_n^{kl}(s)$ $(n = 1, \ldots, N_k)$, respectively. The coefficients $A_n^{kl}(s)$ and $B_n^{kl}(s)$, involved in expression (13), are found in vector form as

$$\mathbf{A}^{kl}(s) = -\mathbf{F}^{kl}(s)\mathbf{Y}^l(s); \quad \mathbf{B}^{kl}(s) = -\mathbf{G}^{kl}(s)\mathbf{Z}^l(s) \quad (15)$$

where $\mathbf{F}^{kl}(s)$ is a $(N_k+1)\times(N_l+1)$-dimensional matrix and $\mathbf{G}^{kl}(s)$ is a $N_k \times N_l$-dimensional matrix, defined in Appendix A. Note that in expressions (15) and in what follows, a repeated index does not imply summation.

Using the orthogonal properties of Fourier series, we can reformulate Eq. (12) in vector form as

$$\mathbf{Y}^k(s) + \mathbf{A}^{kl}(s) = \frac{1}{s}\mathbf{c}^k; \quad \mathbf{Z}^k(s) + \mathbf{B}^{kl}(s) = \frac{1}{s}\mathbf{d}^k \quad (16)$$

where we introduced the (N_k+1)-dimensional vector of Fourier coefficients $\mathbf{c}^k$ and the N_k-dimensional vector of Fourier coefficients $\mathbf{d}^k$ of the form (14) with $\boldsymbol{\Upsilon}_{N_k+1} = \mathbf{c}^k$ and $\Upsilon_n = c_n^k$ $(n = 0, \ldots, N_k)$, and $\boldsymbol{\Upsilon}_{N_k} = \mathbf{d}^k$ and $\Upsilon_n = d_n^k$ $(n = 1, \ldots, N_k)$, respectively.

[1] Not to be confused with the temperature $T(x,t)$.

With the use of expressions (15), Eqs. (16) yield

$$\mathbf{Y}^k(s) - \mathbf{F}^{kl}(s)\mathbf{Y}^l(s) = \frac{1}{s}\mathbf{c}^k; \quad \mathbf{Z}^k(s) - \mathbf{G}^{kl}(s)\mathbf{Z}^l(s) = \frac{1}{s}\mathbf{d}^k \quad (17)$$

A combination of Eqs. (17) for $k = 1, 2$ allows one to separate vectors $\mathbf{Y}^k(s)$ and $\mathbf{Y}^l(s)$, or vectors $\mathbf{Z}^k(s)$ and $\mathbf{Z}^l(s)$, and formulate the following equations for the unknown vectors $\mathbf{Y}^k(s)$ and $\mathbf{Z}^k(s)$:

$$\mathbf{U}^k(s)\mathbf{Y}^k(s) = \frac{1}{s}\mathbf{u}^k(s); \quad \mathbf{V}^k(s)\mathbf{Z}^k(s) = \frac{1}{s}\mathbf{v}^k(s) \quad (18)$$

where the matrices $\mathbf{U}^k(s)$, $\mathbf{V}^k(s)$ and vectors $\mathbf{u}^k(s)$, $\mathbf{v}^k(s)$ are given by

$$\mathbf{U}^k(s) = \mathbf{I}_{N_k+1} - \mathbf{F}^{kl}(s)\mathbf{F}^{lk}(s); \quad \mathbf{u}^k(s) = \mathbf{c}^k + \mathbf{F}^{kl}(s)\mathbf{c}^l \quad (19)$$

$$\mathbf{V}^k(s) = \mathbf{I}_{N_k} - \mathbf{G}^{kl}(s)\mathbf{G}^{lk}(s); \quad \mathbf{v}^k(s) = \mathbf{d}^k + \mathbf{G}^{kl}(s)\mathbf{d}^l \quad (20)$$

and $\mathbf{I}_N$ is the $(N \times N)$-dimensional identity matrix.

Eqs. (18) represent temporal systems of N_k+1 and N_k linear equations $(k = 1, 2)$. Formally, vectors $\mathbf{Y}^k(s)$ and $\mathbf{Z}^k(s)$ can be expressed as

$$\mathbf{Y}^k(s) = \frac{1}{s}[\mathbf{U}^k(s)]^{-1}\mathbf{u}^k(s); \quad \mathbf{Z}^k(s) = \frac{1}{s}[\mathbf{V}^k(s)]^{-1}\mathbf{v}^k(s) \quad (21)$$

Substituting solutions (21) for the unknown Fourier coefficients into expression (11), the transformed temperature $\widehat{T}_k(x,s)$ is obtained in the form

$$\widehat{T}_k(x,s) = [\mathbf{a}^k(x,s)]^{\mathrm{T}}\mathbf{Y}^k(s) + [\mathbf{b}^k(x,s)]^{\mathrm{T}}\mathbf{Z}^k(s) \quad (22)$$

where the vectors $\mathbf{a}^k(x,s)$ and $\mathbf{b}^k(x,s)$ are given by

$$\mathbf{a}^k(x,s) = \begin{pmatrix} \frac{K_0(r_k q)}{K_0(R_k q)} \\ \frac{K_1(r_k q)}{K_1(R_k q)}\cos(\varphi_k) \\ \cdots \\ \frac{K_{N_k}(r_k q)}{K_{N_k}(R_k q)}\cos(N_k\varphi_k) \end{pmatrix}; \quad \mathbf{b}^k(x,s) = \begin{pmatrix} \frac{K_1(r_k q)}{K_1(R_k q)}\sin(\varphi_k) \\ \cdots \\ \frac{K_{N_k}(r_k q)}{K_{N_k}(R_k q)}\sin(N_k\varphi_k) \end{pmatrix} \quad (23)$$

The final solution $\widehat{T}(x,s)$ is the following:

$$\widehat{T}(x,s) = \frac{1}{s}\sum_{k=1}^{2}\{[\mathbf{a}^k(x,s)]^{\mathrm{T}}[\mathbf{U}^k(s)]^{-1}\mathbf{u}^k(s) + [\mathbf{b}^k(x,s)]^{\mathrm{T}}[\mathbf{V}^k(s)]^{-1}\mathbf{v}^k(s)\} \quad (24)$$

4. Solution in the time domain

To obtain the temperature $T(x,t)$ in the time domain, we apply the following complex inversion formula [6]:

$$T(x,t) = \frac{1}{2\pi \mathrm{i}}\int_{\sigma-\mathrm{i}\infty}^{\sigma+\mathrm{i}\infty} \mathrm{e}^{st}\widehat{T}(x,s)\mathrm{d}s \quad (25)$$

where a real number σ should be chosen such that all singularities of the function $\widehat{T}(x,s)$ are located to the left of

the vertical line $\mathrm{Re}(s)=\sigma$. We change the contour of integration in formula (25) as done in [6] for similar problems (Sections 12.3 and 13.5). The new integration contour includes two semi-infinite lines parameterized as $s=u^2\mathrm{e}^{\pm\mathrm{i}\pi}, u\in(0,\infty)$ (with opposite directions of travel) and a vanishingly small circle centered at $s=0$ (with a counter-clockwise direction of integration). The solution $T(x,t)$ is then obtained as

$$T(x,t)=T_s(x)-\frac{2}{\pi}\int_0^\infty u\mathrm{e}^{-u^2t}\mathrm{Im}[\widehat{T}(x,u^2\mathrm{e}^{\mathrm{i}\pi})]\mathrm{d}u \tag{26}$$

where the term $T_s(x)$ is defined in Appendix C, and the symbol Im[ ] denotes the imaginary part of a complex number. As seen from Eq. (26), the computation of the temperature $T(x,t)$ involves the computation of the transformed solution $\widehat{T}(x,s)$ at points $s=u^2\mathrm{e}^{\mathrm{i}\pi}$, for $u\in(0,\infty)$.

The term $T_s(x)$ involved in Eq. (26) represents a semi-analytical solution for the steady-state temperature,

$$T_s(x)=\lim_{t\to\infty}T(x,t) \tag{27}$$

which is the solution of the Laplace's equation corresponding to the steady-state heat conduction problem. An analytical solution to this problem was obtained in [6] using bipolar coordinates. For various cases of boundary conditions $\Phi_k(\varphi_k)$, we have tested that our semi-analytical steady-state solution $T_s(x)$ converges to the analytical solution as $N_1,N_2\to\infty$.

The normal flux at the boundary of the kth cavity can be found using the transformed solution $\widehat{T}(x,s)$. The Laplace transform of the boundary flux can be found by differentiating the transformed temperature $\widehat{T}(x,s)$ with respect to r_k and setting $r_k=R_k$. Using expressions (23) and (24), such derivatives are easy to obtain. After that, an inverse Laplace transform may be applied to the transformed flux in the same way as it is done in Eqs. (25) and (26). The final expression for the dimensionless normal flux is obtained as

$$-\left[\frac{\partial T(x,t)}{\partial r_k}\right]_{L_k}=H_k(\varphi_k)+\frac{2}{\pi}\int_0^\infty u\mathrm{e}^{-u^2t}\mathrm{Im}\left[\left[\frac{\partial\widehat{T}(x,u^2\mathrm{e}^{\mathrm{i}\pi})}{\partial r_k}\right]_{L_k}\right]\mathrm{d}u \tag{28}$$

where the first term $H_k(\varphi_k)=-[\frac{\partial T_s(x)}{\partial r_k}]_{L_k}$, which represents the boundary flux corresponding to the steady-state temperature $T_s(x)$, is given in Appendix C.

Expressions (26) and (28) may be further simplified by substituting the expression for the function $\widehat{T}(x,u^2\mathrm{e}^{\mathrm{i}\pi})$ and its derivatives. After a rearrangement of terms, we find that these expressions represent sums of the truncated Fourier series in angles φ_k $(k=1,2)$ with time-dependent coefficients. It can be shown that for fixed numbers N_k $(k=1,2)$, the infinite integrals involved in formulae (26) and (28) converge. Preliminary analysis and numerical results for smooth boundary conditions show that solutions (26) and (28) converge as $N_k\to\infty$.

5. Large-time asymptotic series

To derive a large-time asymptotic formula for the temperature, we use the technique described by Carslaw and Jaeger [6]. It can be shown that the large-time asymptotic formula for the solution $T(x,t)$ may be derived from the series expansion of the solution $\widehat{T}(x,s)$ in the Laplace domain as the transform parameter s tends to zero. Such a series for the solution $\widehat{T}(x,s)$ is presented below. It involves only elementary functions of s, which makes it possible to perform an analytical inversion of the Laplace transform. As a result, the large-time asymptotic formula for the solution $T(x,t)$ is obtained in a closed form.

5.1. Series for the solution in the Laplace domain ($s\to 0$)

It is found that the series for the transformed solution $\widehat{T}(x,s)$ has the following form:

$$\widehat{T}(x,s)=\frac{T_s(x)}{s}+\sum_{m=1}^{M_0}\frac{A_{0m}(x)}{s(\ln s)^m}+\sum_{m=-2}^{M_1}\frac{A_{1m}(x)}{(\ln s)^m}+R(s,M_0,M_1) \tag{29}$$

where $T_s(x)$ is the steady-state solution (see Section 4); coefficients $A_{pm}(x)$ $(p=0,1)$ are listed in Appendix B.4; the numbers of terms M_0 and M_1 in the summations are discussed below, and the remainder $R(s,M_0,M_1)$ is of the order

$$R(s,M_0,M_1)=\mathrm{O}\left(\frac{1}{s(\ln s)^{M_0+1}}\right)+\mathrm{O}\left(\frac{1}{(\ln s)^{M_1+1}}\right)+\mathrm{O}(s\ln^3 s) \tag{30}$$

The derivation of series (29) is based on the series expansions of the vectors and inverse matrices involved in expression (24) as $s\to 0$. The components of the vectors involve combinations of modified Bessel functions for which such expansions are available [21]. For example, series for the vectors $\mathbf{a}^k(x,s)$ and $\mathbf{b}^k(x,s)$ have the following form:

$$\mathbf{a}^k(x,s)=\sum_{p=0}^{1}\sum_{m=-p}^{M_p}\frac{s^p}{(\ln s)^m}\mathbf{a}^k_{pm}(x)+\mathbf{R}_1(s,M_0,M_1) \tag{31}$$

$$\mathbf{b}^k(x,s)=\mathbf{b}^k_{00}(x)+s\mathbf{b}^k_{10}(x)+s\ln s\mathbf{b}^k_{1,-1}(x)+\mathrm{O}(s^2\ln^2 s) \tag{32}$$

where the vector coefficients $\mathbf{a}^k_{pm}(x)$ and $\mathbf{b}^k_{pm}(x)$ are listed in Appendix B.1, and the remainder $\mathbf{R}_1(s,M_0,M_1)$ is of the order

$$\mathbf{R}_1(s,M_0,M_1)=\mathrm{O}\left(\frac{1}{(\ln s)^{M_0+1}}\right)+\mathrm{O}\left(\frac{s}{(\ln s)^{M_1+1}}\right)+\mathrm{O}(s^2\ln^2 s) \tag{33}$$

Series for the vectors $\mathbf{u}^k(s)$ and $\mathbf{v}^k(s)$, obtained similarly as (31) and (32), are given in Appendix B.2.

It is more difficult to obtain series for the inverse matrices $[\mathbf{U}^k(s)]^{-1}$ and $[\mathbf{V}^k(s)]^{-1}$ involved in expression (24), inasmuch as there is no simple formula for the inverse of a

matrix of arbitrary dimensions. An additional difficulty arises because of the non-invertibility of the matrix $\mathbf{U}^k(s)$ at $s = 0$. To obtain series for the inverse matrices, the following procedure was adopted.

First, the analysis was performed for the matrices of small dimensions for which it was possible to derive the expansions explicitly (for 2×2 matrices) or obtain the expansions using the symbolic computations software Mathematica (for $N \times N$ matrices with $N = 3, 4, 5$). In each case, the expansions of the inverse matrices had the following form

$$[\mathbf{U}^k(s)]^{-1} = \sum_{p=0}^{1} \sum_{m=-p-1}^{M_p} \frac{s^p}{(\ln s)^m} \widetilde{\mathbf{U}}^k_{pm} + \mathbf{R}_5(s, M_0, M_1) \tag{34}$$

$$[\mathbf{V}^k(s)]^{-1} = \widetilde{\mathbf{V}}^k_{00} + s\widetilde{\mathbf{V}}^k_{10} + s\ln s\widetilde{\mathbf{V}}^k_{1,-1} + \mathrm{O}(s^2\ln^2 s) \tag{35}$$

where the remainder $\mathbf{R}_5(s, M_0, M_1)$ is of the order given by expression (33); the first term in series (34) is a singular logarithmic term ($\ln s\,\widetilde{\mathbf{U}}^k_{0,-1}$), and the first term in series (35) is a scalar matrix $\widetilde{\mathbf{V}}^k_{00} = [\mathbf{V}^k(0)]^{-1}$ (matrix $\mathbf{V}^k(0)$ is invertible).

Based on the analysis of the corresponding expansions of the direct matrices $\mathbf{U}^k(s)$ and $\mathbf{V}^k(s)$, we made the assumption that the expansions of the inverse matrices $[\mathbf{U}^k(s)]^{-1}$ and $[\mathbf{V}^k(s)]^{-1}$ of arbitrary dimensions have the form (34) and (35).

To find the unknown matrix coefficients $\widetilde{\mathbf{U}}^k_{pm}$ and $\widetilde{\mathbf{V}}^k_{pm}$ involved in expansions (34) and (35), we consider the matrix equations

$$\mathbf{U}^k(s)[\mathbf{U}^k(s)]^{-1} = \mathbf{I}_{N_k+1}; \quad \mathbf{V}^k(s)[\mathbf{V}^k(s)]^{-1} = \mathbf{I}_{N_k} \tag{36}$$

We expand the matrices $\mathbf{U}^k(s)$ and $\mathbf{V}^k(s)$ using the expansions of the involved Bessel functions, as follows:

$$\mathbf{U}^k(s) = \sum_{p=0}^{1} \sum_{m=-p}^{M_p} \frac{s^p}{(\ln s)^m} \mathbf{U}^k_{pm} + \mathbf{R}_2(s, M_0, M_1) \tag{37}$$

$$\mathbf{V}^k(s) = \mathbf{V}^k_{00} + s\mathbf{V}^k_{10} + s\ln s\mathbf{V}^k_{1,-1} + \mathrm{O}(s^2\ln^2 s) \tag{38}$$

where the matrix coefficients $\mathbf{U}^k_{pm}$ and $\mathbf{V}^k_{pm}$ are discussed in Appendix B.3, and the remainder $\mathbf{R}_2(s, M_0, M_1)$ is of the order given by expression (33). With the use of expansions (34), (35), (37) and (38), Eqs. (36) yield

$$\ln s(\mathbf{U}^k_{00}\widetilde{\mathbf{U}}^k_{0,-1}) + (\mathbf{U}^k_{00}\widetilde{\mathbf{U}}^k_{00} + \mathbf{U}^k_{01}\widetilde{\mathbf{U}}^k_{0,-1}) + \frac{1}{\ln s}(\mathbf{U}^k_{00}\widetilde{\mathbf{U}}^k_{01} + \cdots) + \ldots = \mathbf{I}_{N_k+1} \tag{39}$$

$$\mathbf{V}^k_{00}\widetilde{\mathbf{V}}^k_{00} + s(\mathbf{V}^k_{00}\widetilde{\mathbf{V}}^k_{10} + \mathbf{V}^k_{10}\widetilde{\mathbf{V}}^k_{00}) + s\ln s(\mathbf{V}^k_{00}\widetilde{\mathbf{V}}^k_{1,-1} + \mathbf{V}^k_{1,-1}\widetilde{\mathbf{V}}^k_{00}) + \cdots = \mathbf{I}_{N_k} \tag{40}$$

where the terms of the same orders in s are collected together.

Since the right-hand sides of Eqs. (39) and (40) are s-independent, all s-dependent terms in the left-hand sides of these equations must be zero, and the s-independent terms in the left-hand sides must be equal to the identity matrices from the right-hand sides. These conditions lead to linear equations for the unknown matrices $\widetilde{\mathbf{U}}^k_{pm}$ and $\widetilde{\mathbf{V}}^k_{pm}$.

Although Eqs. (39) and (40) look similar, there is a major difference in the solution of these equations. The solution of Eq. (40) for the matrices $\widetilde{\mathbf{V}}^k_{pm}$ is straightforward since the matrix $\mathbf{V}^k_{00} = \mathbf{V}^k(0)$ is invertible (see Appendix B.3). The solution of Eq. (39) for the matrices $\widetilde{\mathbf{U}}^k_{pm}$ is more complicated since the matrix $\mathbf{U}^k_{00} = \mathbf{U}^k(0)$ is non-invertible. To solve Eq. (39), one needs to deal with the problem of an underdetermined linear system of equations, which can be resolved using the *annihilation principle* [22].

For example, the first matrix equation deduced from Eq. (39) is the following:

$$\mathbf{U}^k_{00}\widetilde{\mathbf{U}}^k_{0,-1} = \mathbf{0} \tag{41}$$

where we put the null matrix $\mathbf{0}$ in the right-hand side. The linear system corresponding to Eq. (41) is *underdetermined*, in the sense that the number of the linearly independent equations is less than the number of the unknowns (components of the matrix $\widetilde{\mathbf{U}}^k_{0,-1}$). To complete this system, additional conditions must be imposed on the unknown matrix $\widetilde{\mathbf{U}}^k_{0,-1}$.

The missing equations can be derived from the second matrix equation

$$\mathbf{U}^k_{00}\widetilde{\mathbf{U}}^k_{00} + \mathbf{U}^k_{01}\widetilde{\mathbf{U}}^k_{0,-1} = \mathbf{I}_{N_k+1} \tag{42}$$

which is deduced from the second term in the left-hand side expansion in Eq. (39). Eq. (42) involves the term $\mathbf{U}^k_{00}\widetilde{\mathbf{U}}^k_{00}$ where the matrix $\widetilde{\mathbf{U}}^k_{00}$ is unknown too. To eliminate this term, the $(N_k + 1)$-dimensional *annihilating vector* $\mathbf{n}^k$ is introduced, such that it satisfies the underdetermined linear system $[\mathbf{n}^k]^{\mathrm{T}}\mathbf{U}^k_{00} = \mathbf{0}$. For convenience, we choose $\mathbf{n}^k$ such that its first component is equal to 1. Operating with the transposed vector $[\mathbf{n}^k]^{\mathrm{T}}$ on both sides of Eq. (42), we eliminate the term $\mathbf{U}^k_{00}\widetilde{\mathbf{U}}^k_{00}$ and obtain the corresponding equation

$$[\mathbf{n}^k]^{\mathrm{T}}\mathbf{U}^k_{01}\widetilde{\mathbf{U}}^k_{0,-1} = [\mathbf{n}^k]^{\mathrm{T}} \tag{43}$$

Eq. (43) contains the missing equations for the matrix $\widetilde{\mathbf{U}}^k_{0,-1}$. As a result, this matrix can be found as a solution to the linear system composed of linearly independent equations from the systems (41) and (43).

The same routine is used to find the rest of the matrices $\widetilde{\mathbf{U}}^k_{pm}$. For each matrix, we impose two simultaneous matrix equations, deduced from the consecutive terms in the left-hand side expansion in Eq. (39). One of the matrix equations represents an underdetermined linear system, and the other matrix equation is used to retrieve the missing equations. The annihilating vector is used to eliminate additional unknowns involved in the latter matrix equation. The final linear system is composed of linearly independent equations, retrieved from the two simultaneous matrix equations. More details on the use of the annihilation principle can be found in the work of Kruskal [22]. The resulting equations for the matrices $\widetilde{\mathbf{U}}^k_{pm}$ are listed in Appendix B.3.

To verify the validity of expansions (34) and (35), we compared the inverse matrices obtained using numerical

inversion procedures with the matrices obtained using series (34) and (35), for various values of the involved parameters. A good agreement of the results was obtained in each case. This allows us to suggest that series (34) and (35) can be used for arbitrary numbers N_k.

Finally, the expansions obtained for the vectors and matrices are substituted into formula (24) for the transformed solution $\widehat{T}(x,s)$. Series (29) is obtained by multiplying the substituted expansions and collecting together the terms of the same orders in s.

5.2. Series for the solution in the time domain

The asymptotic series for the temperature $T(x,t)$ is obtained by applying the inverse Laplace transform to series (29) and integrating the series term by term. The integration of series (29) is performed with the help of integral formulae presented in [6] (p. 340) and asymptotic formulae for some of the involved integrals given in [23]. As the result, the asymptotic series for the temperature $T(x,t)$ for large t is obtained in the form

$$T(x,t) = T_s(x) + \sum_{m=1}^{M_0} \frac{\Lambda_{0m}(x)}{(\ln t)^m} + \frac{1}{t}\sum_{m=-1}^{M_1} \frac{\Lambda_{1m}(x)}{(\ln t)^m} + \epsilon(t, M_0, M_1) \tag{44}$$

where the coefficients $\Lambda_{pm}(x)$ $(p = 0, 1)$ are listed in Appendix D, and the remainder $\epsilon(t, M_0, M_1)$ is of the order

$$\epsilon(t, M_0, M_1) = \mathrm{O}\left(\frac{1}{(\ln t)^{M_0+1}}\right) + \mathrm{O}\left(\frac{1}{t(\ln t)^{M_1+1}}\right) + \mathrm{O}\left(\frac{\ln^2 t}{t^2}\right) \tag{45}$$

The numbers M_0, M_1 should be chosen for each specific t such that all three terms in remainder (45) are of approximately same order. In the numerical examples presented in this paper, we used $M_0 = 6$, $M_1 = 2$. With these values of M_0 and M_1, each term in expression (45) does not exceed 10^{-6} for $t \geqslant 10^4$.

In addition to providing an approximation for the temperature $T(x,t)$ for large values of t, series (44) can be used to estimate the rate of convergence of $T(x,t)$ to its limiting steady-state value $T_s(x)$ as $t \to \infty$. For example, the first term in the summation in expression (44) gives the following estimate:

$$T(x,t) - T_s(x) \approx \frac{\Lambda_{01}(x)}{\ln t}, \quad t \to \infty \tag{46}$$

which states that the difference $T(x,t) - T_s(x)$ is of the order $(\ln t)^{-1}$. It can be shown that if prescribed boundary conditions are skew-symmetric with respect to the line connecting the centers of the cavities (the case when for each k the prescribed boundary temperature $\Phi_k(\varphi_k)$ is an odd function of polar angle φ_k and its Fourier coefficients c_n^k are zero for all n), then the coefficients $\Lambda_{0m}(x)$ $(m \geqslant 1)$ and $\Lambda_{1,-1}(x)$ in series (44) are zero, and the difference $T(x,t) - T_s(x)$ is of the order t^{-1}.

The asymptotic series for the heat flux at the boundary L_k can be obtained by differentiating series (29) with respect to r_k, setting $r_k = R_k$, and then applying the inverse Laplace transform, similarly as done to obtain series (44).

6. Numerical implementation

The numerical computation of the temperature $T(x,t)$ consists of two parts: (1) determination of the numbers N_k $(k = 1, 2)$ needed to achieve a specified accuracy level, and (2) computation of the temperature $T(x,t)$ at specified points $x = x_1, \ldots, x_m$, at non-zero time instants $t = t_1, \ldots, t_n$. Details of these steps are described below.

6.1. Determination of the numbers of terms in the Fourier series

The numbers N_k should be chosen such that the temperature $T(x,t)$ will satisfy boundary conditions (4) up to a predefined accuracy level ε, that is

$$\max_{-\pi<\varphi_k\leqslant\pi} |T(x,t)|_{L_k} - \Phi_k(\varphi_k)| < \varepsilon, \quad k = 1, 2 \tag{47}$$

The boundary error $|T(x,t)|_{L_k} - \Phi_k(\varphi_k)|$ may be estimated as follows:

$$|T(x,t)|_{L_k} - \Phi_k(\varphi_k)| \leqslant |T(x,t) - T_s(x)|_{L_k} + |T_s(x)|_{L_k} - \Phi_k(\varphi_k)| \tag{48}$$

where the second term $|T_s(x)|_{L_k} - \Phi_k(\varphi_k)|$ is t-independent and represents the boundary error in the steady-state solution $T_s(x)$. In numerical examples, it has been seen that the leading term in expression (48) is the steady-state term $|T_s(x)|_{L_k} - \Phi_k(\varphi_k)|$, and that the numerical value of expression (47) does not change much with the increase in time t.

Based on these considerations, the numbers N_k are first chosen such that the steady-state boundary error $|T_s(x)|_{L_k} - \Phi_k(\varphi_k)|$ does not exceed the accuracy limit ε for each k. This is done using an iterative algorithm, where the numbers N_k are increasing until the maximum of the error $|T_s(x)|_{L_k} - \Phi_k(\varphi_k)|$, computed at a number (say, 360) of equally spaced points x along the boundaries L_k, is less than ε. (If the problem is symmetric with respect to the line connecting the centers of the cavities (which is the case when $\mathbf{d}^k = 0$, $k = 1, 2$), boundary points may be equally spaced along only one symmetric part of each boundary L_k.)

After that, the numbers N_k are adjusted such that the error of the transient solution $|T(x,t_1) - \Phi_k(\varphi_k)|$ at the minimum specified time instant $t = t_1$ does not exceed the accuracy limit ε for each k. The numbers N_k are iteratively increased until the maximum of the error $|T(x,t_1) - \Phi_k(\varphi_k)|$, computed at equally spaced points x along the boundaries L_k, is less than ε.

In numerical tests run to date, the numbers N_k computed using the steady-state boundary error $|T_s(x)|_{L_k} - \Phi_k(\varphi_k)|$ in almost all cases guaranteed that the boundary

error of the transient solution $|T(x,t_1)-\Phi_k(\varphi_k)|$ for different values of t_1 is less than ε.

6.2. Computation of the solution

As soon as the numbers N_k are chosen, temperature $T(x,t)$ can be computed at points $x=x_1,\dots,x_m$, at times $t=t_1,\dots,t_n$. We discuss below the computation of the temperature for small and intermediate values of t. For large values of t, asymptotic series (44) is used. The range of validity of the asymptotic series is discussed in Section 7.

The steady-state solution $T_s(x)$ at points $x=x_1,\dots,x_m$ is computed according to the formula given in Appendix C. The computation of the transient term in temperature $T(x,t)$ involves the integration over an infinite interval (see Eq. (26)), where the computation of the integrand function involves matrix inversions (see Eq. (24)).

The integrand function in Eq. (26), corresponding to points $x=x_1,\dots,x_m$ and times $t=t_1,\dots,t_n$, may be represented as a matrix-function $f(u)$ with a matrix (m,n)-element $f_{mn}(u)$ as follows:

$$f_{mn}(u)=u\mathrm{e}^{-u^2t_n}\mathrm{Im}[\widehat{T}(x_m,s)]_{s=u^2\mathrm{e}^{\mathrm{i}\pi}} \tag{49}$$

To evaluate the term $\widehat{T}(x_m,s)$ involved in expression (49), we use expression (24). The inverse matrices $[\mathbf{U}^k(s)]^{-1}$ and $[\mathbf{V}^k(s)]^{-1}$ involved in expression (24) can be computed just once for each value of the integration variable u ($s=u^2\mathrm{e}^{\mathrm{i}\pi}$). The integration of the matrix-function $f(u)$ may be then performed row by row, or column by column, using available quadratures for the integrals of the vector-functions. In the numerical examples presented in this paper, the solution was computed separately for each time instant t_n by integrating the corresponding columns of the matrix $f(u)$.

The integral of the function $f(u)$ over the infinite interval can be split into two integrals:

$$\int_0^\infty f(u)\mathrm{d}u=\int_0^\delta f(u)\mathrm{d}u+\int_\delta^\infty f(u)\mathrm{d}u \tag{50}$$

where $0<\delta<\infty$. The integration over the interval $(0,\delta)$ is performed using the expansion of the integrand function $f(u)$ in series in u in the vicinity of $u=0$. Such an expansion is obtained using expansion (29) of the transformed temperature $\widehat{T}(x,s)$. The typical terms that appear in the series for $f(u)$ involve combinations of positive and negative powers of u and $\ln u$, which makes it possible to perform the integration over the interval $(0,\delta)$ analytically or using simple quadrature rules. As a result, no matrix inversion is needed for integration over the interval $(0,\delta)$. The choice of an appropriate value of δ is based on the analysis of the error introduced by approximating the function $f(u)$ using the series expansion. In the numerical examples presented below (see Section 7), δ is chosen as $\delta=10^{-5}t^{-1/2}$ if $t\geqslant 1$ and $\delta=10^{-5}$ if $t<1$.

The integration over the interval (δ,∞) is performed numerically using a change of the integration variable to transform the infinite integration interval into a finite one. This kind of transformation is automatically exploited in available routines created for the numerical computation of integrals over infinite intervals (see, for example, [24]). The inverse matrices involved in the integrand function $f(u)$ can be computed using standard linear solvers.

To reduce the computational cost of matrix inversions, we adopted an iterative procedure based on an alternating algorithm [25]. In this algorithm, the unknown boundary value $\widehat{T}_k(x,s)|_{L_k}$ and the unknown vectors of its Fourier coefficients $\mathbf{Y}^k(s)$ and $\mathbf{Z}^k(s)$ (Eq. (11)) are adjusted iteratively to account for the cavities interactions. As a result, the inverse matrices $[\mathbf{U}^k(s)]^{-1}$ and $[\mathbf{V}^k(s)]^{-1}$ are approximated by the following Neumann series

$$\mathbf{U}^{k,M}(s)=\mathbf{I}_{N_k+1}+\sum_{m=1}^{M-1}(\mathbf{F}^{kl}(s)\mathbf{F}^{lk}(s))^m \tag{51}$$

$$\mathbf{V}^{k,M}(s)=\mathbf{I}_{N_k}+\sum_{m=1}^{M-1}(\mathbf{G}^{kl}(s)\mathbf{G}^{lk}(s))^m \tag{52}$$

where M is the number of steps in the alternating algorithm. The choice of the number M for a specific time t at which $T(x,t)$ is computed is performed iteratively to guarantee a sufficiently accurate approximation of the boundary temperature $\Phi_k(\varphi_k)$ by the transient solution $T(x,t)$. The algorithm is similar to the one described in Section 6.1. It has been observed in numerical tests that M increases with an increase in t, and it may increase with an increase in numbers N_k $(k=1,2)$. Preliminary analytical and numerical results have shown that the solution $T(x,t)$ obtained using the alternating algorithm converges to the solution obtained using standard linear solvers, but a strict mathematical proof of convergence is lacking.

7. Numerical examples

In this section we consider two examples corresponding to uniform and non-uniform boundary temperature. In both examples, zero dimensionless temperature $T(x,t)|_{L_2}=0$ is prescribed at the boundary L_2. For simplicity, the numbers of terms in the Fourier series N_k $(k=1,2)$ were chosen equal, i.e. $N_1=N_2$.

7.1. Uniform boundary temperature

Unit dimensionless temperature $T(x,t)|_{L_1}=1$ is prescribed at the boundary L_1. The problem is solved for the cases when $R_1=0.2,\ 0.3,\ 0.5,\ 0.6$ and $R_2=0.3$. In Table 1 we present our results for the dimensionless temperature $T(x,t)$ and the steady-state temperature $T_s(x)$ calculated at two points, point A and point B, defined as $A=(1.5\rho,\pi)$, $B=(2.5\rho,0)$ in polar coordinates $(\rho r_1,\varphi_1)$ and as $A=(2.5\rho,\pi)$, $B=(1.5\rho,0)$ in polar coordinates $(\rho r_2,\varphi_2)$ (see Fig. 2). The temperature $T(x,t)$ was computed at times $t=1,\ 10,\ 100$.

The predetermined accuracy level ε and the numbers N_1 and M (M is the number of steps in the alternating

Table 1
Temperature $T(x,t)$ and steady-state temperature $T_s(x)$ at points A and B in Fig. 2

ε	R_1	N_1		$t=1$	$t=10$	$t=100$	$T_s(x)$
10^{-6}	0.2	9		$M=10$	$M=15$	$M=19$	–
			A	0.15440	0.34789	0.43136	0.60023
			B	0.00606	0.06030	0.11658	0.27223
10^{-6}	0.3	10		$M=20$	$M=20$	$M=22$	–
			A	0.20006	0.41523	0.50605	0.68454
			B	0.00847	0.07453	0.14011	0.31546
10^{-6}	0.5	20		$M=20$	$M=23$	$M=38$	–
			A	0.29869	0.53339	0.62918	0.80787
			B	0.01528	0.10614	0.18788	0.39175
10^{-5}	0.6	28		$M=20$	$M=33$	$M=46$	–
			A	0.35287	0.58714	0.68154	0.85353
			B	0.02031	0.12508	0.21427	0.42868

algorithm, see Section 6.2) used to achieve the solution according to this accuracy level are reported in the table. In most computations performed for these examples we adopted the predetermined accuracy level $\varepsilon = 10^{-6}$. For the case when the boundaries of the cavities were close to each other, we had to relax the conditions on the predetermined accuracy level and took it to be $\varepsilon = 10^{-5}$ for the case $R_1 = 0.6$.

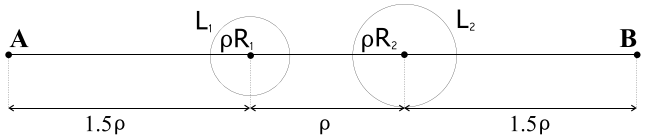

Fig. 2. Location of points A and B.

The values of the temperature $T(x,t)$ presented in the table coincided with the values obtained using the finite element method to within 4 or 5 significant digits. The finite element method results were obtained using the commercial software COMSOL Multiphysics (formerly known as FEMLAB). The values of the steady-state temperature $T_s(x)$ coincided with the analytical solution given in [6] to 6 or more significant digits.

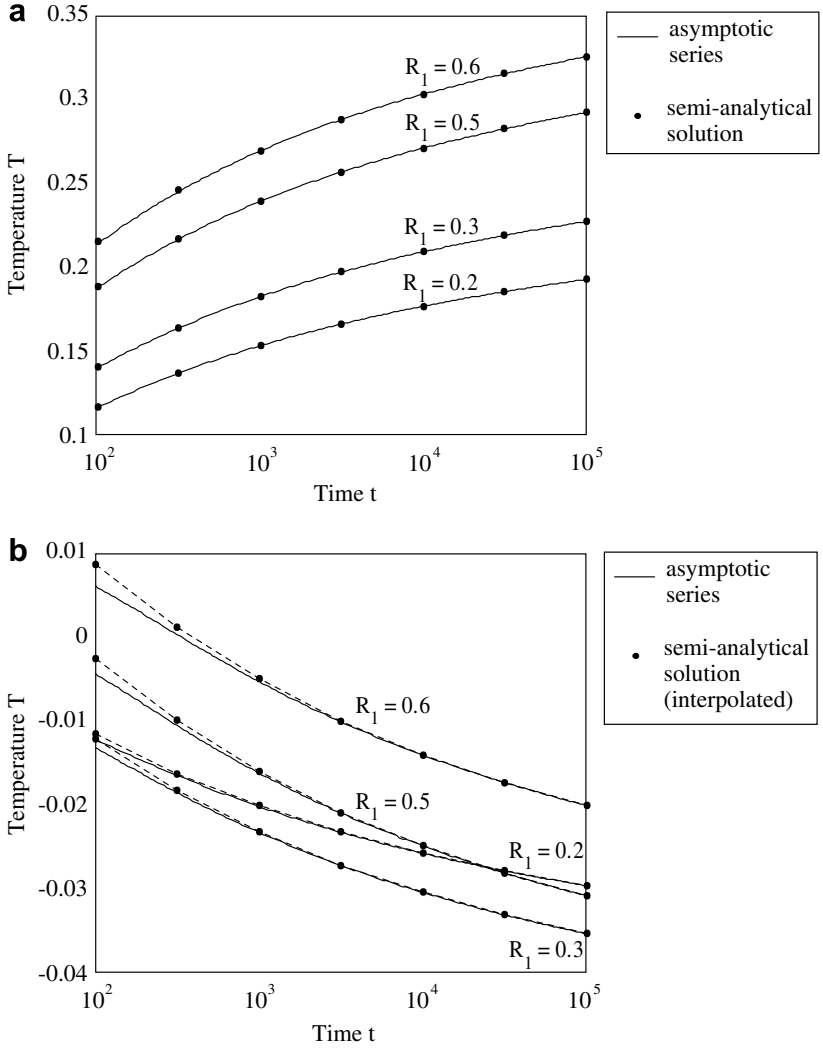

Fig. 3. The distribution of the dimensionless temperature $T(x,t)$ at point B (see Fig. 2) over the time interval $10^2 \leqslant t \leqslant 10^5$ for uniform (a) and non-uniform (b) prescribed temperature $T(x,t)|_{L_1}$.

For the same geometry, the temperature $T(x,t)$ was computed for large values of time. A comparison of the results obtained using the asymptotic formula (44) with the results obtained using the integral solution (26) is given in Fig. 3a, which shows the distribution of the dimensionless temperature $T(x,t)$ at point B, for times $10^2 \leqslant t \leqslant 10^5$. The continuous curves on the plots show the temperature computed using the asymptotic formula (44). The dots on the plots show the temperature computed using solution (26). It is seen that the results obtained with the asymptotic series are in a good agreement with the results obtained using solution (26). In all the cases, the relative error (defined as the absolute value of the ratio of the difference between the asymptotic and the integral solutions to the value of the integral solution) did not exceed 0.6% and decreased with the increase in time.

7.2. Non-uniform boundary temperature

This example is designed to study the influence of the boundary conditions. The temperature at the boundary L_1 is prescribed as $T(x,t)|_{L_1} = \cos\varphi_1$. We solve this problem for the same values of the parameters involved in the formulation in the previous example. The results are reported in Table 2. As in the previous example, we had to relax the conditions on the predetermined accuracy level for the case $R_1 = 0.6$. A comparison of the results for the temperature at point B at times $10^2 \leqslant t \leqslant 10^5$, obtained using the asymptotic formula (44), with the results obtained using the integral solution (26) is given in Fig. 3b. The relative error at point B decreased with the increase in time as well, even though it was higher than in the previous example. The relative error at point B was at most 30.5% (for the case $R_1 = 0.6$) at time $t = 10^2$, 5% at $t = 10^3$, and 0.2% at $t = 10^4$.

A comparison of the results obtained using our method with the results obtained using the finite element method and the analytical steady-state solution [6] is given in Fig. 4 (for the case $R_1 = 0.6$). Fig. 4 shows the distribution

Table 2
Temperature $T(x,t)$ and steady-state temperature $T_s(x)$ at points A and B in Fig. 2

ε	R_1	N_1		$t=1$	$t=10$	$t=100$	$T_s(x)$
10^{-6}	0.2	10		$M=10$	$M=15$	$M=19$	–
			A	−0.08039	−0.14587	−0.16861	−0.20979
			B	0.00177	−0.00049	−0.01170	−0.04908
10^{-6}	0.3	11		$M=20$	$M=20$	$M=22$	–
			A	−0.12365	−0.21051	−0.23908	−0.28832
			B	0.00298	0.00183	−0.01228	−0.05972
10^{-6}	0.5	20		$M=20$	$M=23$	$M=38$	–
			A	−0.22131	−0.33428	−0.36755	−0.41880
			B	0.00683	0.01293	−0.00278	−0.05944
10^{-5}	0.6	28		$M=20$	$M=33$	$M=46$	–
			A	−0.27677	−0.39575	−0.42881	−0.47642
			B	0.01005	0.02282	0.00826	−0.04870

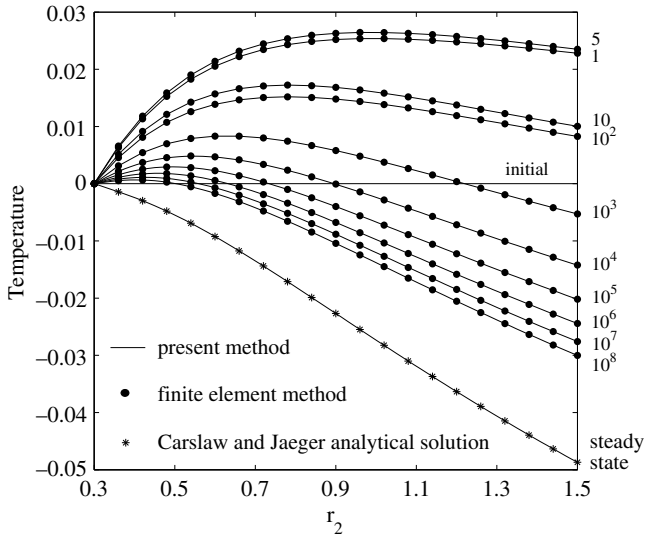

Fig. 4. The distribution of the dimensionless temperature $T(x,t)$ and the steady-state temperature $T_s(x)$ along the horizontal line connecting the boundary L_2 and point B (see Fig. 2). The numbers at the right end of the curves correspond to the moments of dimensionless time $t = 1,\ 5,\ 10,\ 10^2, \ldots, 10^8$.

of the dimensionless temperature $T(x,t)$ for times in the range $t = 1, \ldots, 10^8$ and the steady-state temperature $T_s(x)$ along the horizontal line connecting the boundary L_2 and point B. The temperature is given as a function of the ratio r_2, where $r_2 = 0.3$ corresponds to the point located on the boundary L_2, and $r_2 = 1.5$ corresponds to the point B. Zero initial temperature is shown as well.

The finite element method results were obtained using the software COMSOL Multiphysics. Our results were obtained using solution (26) (for times $t = 1, \ldots, 10^3$) and asymptotic series (44) (for times $t \geqslant 10^4$). For large values of t, the computational time was several seconds using the asymptotic series as opposed to several minutes using the finite element method.

As can be seen from Fig. 4, at small times the temperature at points between the boundary L_2 and point B increases to positive values. At some moment ($t \approx 5$) the temperature reaches its positive maximum and starts to decrease. Finally, it converges to the negative steady state temperature. One can see that it may take as long as $t = 10^8$ for the temperature to reach the steady state. In such cases, it is beneficial to use asymptotic formula (44) to get accurate values of the temperature and to estimate the time at which the temperature is close to its steady-state value.

8. Discussion and conclusions

This paper presents a semi-analytical solution for the transient heat conduction problem of an infinite medium containing two circular cavities. The problem is first solved in the Laplace transform domain using truncated Fourier series approximations of the boundary unknowns and the

addition theorem for the solutions of the governing differential equation. By imposing the boundary condition prescribed for the transformed temperature at the boundary of each cavity and using orthogonality properties of Fourier series, a linear system of equations for the unknown Fourier coefficients is derived. An iterative solution for the linear system is suggested. Application of the analytical inverse Laplace transform results in an integral form of the solution. The asymptotic formula for the solution is obtained using the transformed solution. The asymptotic formula is first obtained in the Laplace transform domain, where it has the form of series involving elementary functions of the transform parameter. An analytical inversion of the Laplace transform is then performed to obtain the asymptotic series for the temperature in the time domain.

The method is capable of accurately computing the temperature and heat flux at any point and any time, without the need to consider a series of discrete time steps, as in conventional numerical procedures. The advantage of the method as opposed to conventional numerical procedures becomes evident when the solution is computed for large values of time.

Several examples are given to demonstrate the validity of the obtained asymptotic formulae. Numerical results show a good agreement of the asymptotic and the integral solutions, as well as a good agreement of our solution and a solution obtained using the finite element method. The convergence of the asymptotic solution to the semi-analytical solution and to the solution obtained using the finite element method has been observed for various values of the parameters involved in the problem. Further analysis should be performed to estimate the error in the solution due to the truncation of Fourier series and to study the convergence of the iterative solution procedure.

The method allows for a direct extension for the problems of multiple cavities and inhomogeneities under various types of linear boundary conditions. Derivation of the solution for these problems follows the main steps of the analysis presented in this paper. However, the case of multiple circular cavities or inhomogeneities will require a significantly more work. As has been shown in the present work, the derivation of the asymptotic solution for the two circular cavities is based on the asymptotic expansions of the singular matrices involved in the problem. Such expansions have been attentively studied using analytical and numerical tools. For the case of multiple circular features, due to the larger dimension of the problem, an accurate asymptotic study of the corresponding singular matrices will not be a simple task. For this reason, the case of two cavities presented here is believed to be of particular importance for further developments.

Acknowledgements

The authors are grateful to Prof. A. Peirce (Department of Mathematics, The University of British Columbia, Canada) who suggested to use the annihilation principle in the present work (a private communication). The authors are also pleased to acknowledge the support of the Minnesota Supercomputing Institute in providing computer time and access to the finite element software COMSOL Multiphysics.

Appendix A. Matrices $\mathbf{F}^{kl}(s)$ and $\mathbf{G}^{kl}(s)$

In what follows (including Appendix B), the indices k, l are reserved to indicate the number of the corresponding cavity. The only possible values of these indices are $k, l = 1, 2$ and $k \neq l$. The vectors are given by their ith elements ($i \geqslant 1$), e.g. $\mathbf{a}^k_{00}(x)(i)$ denotes the ith element of the vector $\mathbf{a}^k_{00}(x)$. The matrices are given by their (i,j)-elements ($i, j \geqslant 1$); e.g. $\mathbf{F}^{kl}(s)(i,j)$ denotes the (i,j) element of the matrix $\mathbf{F}^{kl}(s)$.

Matrices $\mathbf{F}^{kl}(s)$ and $\mathbf{G}^{kl}(s)$ are given by

$$\mathbf{F}^{kl}(s)(i,j) = (-1)^{k(i-1)+l(j-1)+1}\eta_i(K_{i+j-2}(q) + K_{i-j}(q))\frac{I_{i-1}(R_k q)}{K_{j-1}(R_l q)} \tag{53}$$

$$\mathbf{G}^{kl}(s)(i,j) = (-1)^{ki+lj}(K_{i+j}(q) - K_{i-j}(q))\frac{I_i(R_k q)}{K_j(R_l q)} \tag{54}$$

where $I_i(\cdot)$ and $K_i(\cdot)$ are the modified Bessel functions [21]; and $\eta_i = 0.5$ if $i = 1$ and $\eta_i = 1$ if $i \neq 1$.

Appendix B. Coefficients of the series in the Laplace domain

Below, symbols $\binom{m}{n}$ denote the binomial coefficients $\binom{m}{n} = \frac{m!}{n!(m-n)!}$. Constants a_k, α_k, β_k $(k = 1, 2)$ and β are defined as $a_k = r_k/R_k$ and

$$\alpha_k = -\ln\left(\frac{r_k^2}{4}\right) - 2\gamma; \quad \beta_k = -\ln\left(\frac{R_k^2}{4}\right) - 2\gamma;$$
$$\beta = -\ln\left(\frac{1}{4}\right) - 2\gamma \tag{55}$$

where $\gamma = 0.5772\ldots$ is Euler's constant.

B.1. Series for the vectors $\mathbf{a}^k(x,s)$ and $\mathbf{b}^k(x,s)$

The $(N_k + 1)$-dimensional vectors $\mathbf{a}^k_{pm}(x)$ and the N_k-dimensional vectors $\mathbf{b}^k_{pm}(x)$ are given by

$$\mathbf{a}^k_{00}(x)(i) = (a_k)^{1-i}\cos((i-1)\varphi_k) \tag{56}$$

$$\mathbf{a}^k_{0m}(x)(i) = 2\ln(a_k)\beta_k^{m-1}\delta_{1i}, \quad m \geqslant 1 \tag{57}$$

$$\mathbf{a}^k_{1,-1}(x)(i) = R_k^2(4a_k)^{-1}(a_k^2 - 1)\cos(\varphi_k)\delta_{2i} \tag{58}$$

$$\mathbf{a}^k_{10}(x)(i) = \frac{R_k^2\cos((i-1)\varphi_k)}{4(a_k)^{i-1}} \times \begin{cases} 1 + \beta_k - a_k^2(1+\alpha_k) & i = 2 \\ \frac{1}{i-2}(1 - a_k^2) & i \neq 2 \end{cases} \tag{59}$$

$$\mathbf{a}^k_{1m}(x)(i) = 2^{-1}R_k^2\beta_k^{m-2}\left[a_k^2\beta_k(\ln a_k - 1) + 2m\ln a_k + \alpha_k - \beta_k\ln a_k\right]\delta_{1i} \tag{60}$$

where $m \geqslant 1$ in Eq. (60).

$$\mathbf{b}^k_{00}(x)(i) = (a_k)^{-i}\sin(i\varphi_k) \tag{61}$$

$$\mathbf{b}^k_{10}(x)(i) = \frac{R_k^2\sin(i\varphi_k)}{4(a_k)^i} \times \begin{cases} 1+\beta_k - a_k^2(1+\alpha_k) & i=1 \\ \frac{1}{i-1}(1-a_k^2) & i \geqslant 2 \end{cases} \tag{62}$$

$$\mathbf{b}^k_{1,-1}(x)(i) = R_k^2(4a_k)^{-1}(a_k^2-1)\sin(\varphi_k)\delta_{1i} \tag{63}$$

B.2. Series for the vectors $\mathbf{u}^k(s)$ and $\mathbf{v}^k(s)$

Series for the vectors $\mathbf{u}^k(s)$ and $\mathbf{v}^k(s)$ (Eqs. (19) and (20)) are derived using the following expansions of the matrices $\mathbf{F}^{kl}(s)$ and $\mathbf{G}^{kl}(s)$:

$$\mathbf{F}^{kl}(s) = \sum_{p=0}^{1}\sum_{m=-p}^{M_p}\frac{s^p}{(\ln s)^m}\mathbf{F}^{kl}_{pm} + \mathbf{R}_4(s,M_0,M_1) \tag{64}$$

$$\mathbf{G}^{kl}(s) = \mathbf{G}^{kl}_{00} + s\mathbf{G}^{kl}_{10} + s\ln s\mathbf{G}^{kl}_{1,-1} + \mathrm{O}(s^2\ln^2 s) \tag{65}$$

where the remainder $\mathbf{R}_4(s,M_0,M_1)$ is of the order given by expression (33), and the $(N_k+1)\times(N_l+1)$-dimensional matrix coefficients $\mathbf{F}^{kl}_{pm}$ and the $N_k\times N_l$-dimensional matrix coefficients $\mathbf{G}^{kl}_{pm}$ are given below:

$$\mathbf{F}^{kl}_{00}(i,j) = \begin{cases} -\delta_{i1} & j=1 \\ (-1)^{k(i-1)+l(j-1)+1}\dbinom{i+j-3}{i-1}R_k^{i-1}R_l^{j-1} & j\geqslant 2 \end{cases} \tag{66}$$

$$\mathbf{F}^{kl}_{01}(i,j) = \begin{cases} 2\ln(R_l)\delta_{j1} & i=1 \\ (-1)^{k(i-1)}\frac{2}{i-1}R_k^{i-1}\delta_{j1} & i\geqslant 2 \end{cases} \tag{67}$$

$$\mathbf{F}^{kl}_{0m} = \beta_l^{m-1}\mathbf{F}^{kl}_{01}, \quad m\geqslant 2 \tag{68}$$

$$\mathbf{F}^{kl}_{1,-1}(i,j) = (-1)^{k(i-1)+l}4^{-1}R_k^{i-1}R_l(R_l^2+\delta_{i2}-\delta_{i1})\delta_{j2} \tag{69}$$

$$\mathbf{F}^{kl}_{10}(i,j) = \begin{cases} \frac{1}{4}(R_l^2-R_k^2-1)\delta_{i1} + \frac{1}{2}(-1)^k R_k\delta_{i2} \\ \quad j=1 \\ \frac{1}{4}\mathbf{F}^{kl}_{00}(i,j)[R_k^2+R_l^2(1+\beta_l)-(1+\beta)] \\ \quad j=2, \quad i=1 \\ \frac{1}{8}\mathbf{F}^{kl}_{00}(i,j)[R_k^2-2+2R_l^2(1+\beta_l)] \\ \quad j=i=2 \\ \frac{1}{4}\mathbf{F}^{kl}_{00}(i,j)\left[\frac{R_k^2}{i}+\frac{3-i}{(i-1)(i-2)}+R_l^2(1+\beta_l)\right] \\ \quad j=2, \quad i\geqslant 3 \\ \frac{1}{4}\mathbf{F}^{kl}_{00}(i,j)\left[\frac{R_k^2}{i}+\frac{R_l^2}{j-2}+\frac{\delta_{i2}}{(j-1)(j-2)}-\frac{1}{i+j-3}\right] \\ \quad j\geqslant 3 \end{cases} \tag{70}$$

$$\mathbf{F}^{kl}_{1m}(i,j) = \frac{\delta_{j1}}{2}(-1)^{k(i-1)}\beta_l^{m-2}R_k^{i-1} \times \begin{cases} \beta_l(R_k^2\ln R_l+1+\ln R_l)+R_l^2[\ln R_l(2m-\beta_l)-\beta] \\ \quad i=1 \\ \frac{R_k^2}{2}\beta_l-\beta_l(1+2\ln R_l)+R_l^2(2m-2-\beta_l) \\ \quad i=2 \\ \frac{1}{i-1}\left[\frac{R_k^2}{i}\beta_l-\frac{\beta_l}{i-2}+R_l^2(2m-2-\beta_l)\right] \\ \quad i\geqslant 3 \end{cases} \tag{71}$$

where $m\geqslant 1$ in Eq. (71).

$$\mathbf{G}^{kl}_{00}(i,j) = (-1)^{ki+lj}\binom{i+j-1}{i}R_k^iR_l^j \tag{72}$$

$$\mathbf{G}^{kl}_{10}(i,j) = \frac{\mathbf{G}^{kl}_{00}(i,j)}{4} \times \begin{cases} \frac{R_k^2}{2}-1+R_l^2(1+\beta_l) \\ \quad i=j=1 \\ \frac{R_k^2}{i+1}-\frac{1}{i-1}+R_l^2(1+\beta_l) \\ \quad i\geqslant 2, \quad j=1 \\ \frac{R_k^2}{i+1}-\frac{1}{i+j-1}+\frac{R_l^2}{j-1}-\frac{\delta_{i1}}{j(j-1)} \\ \quad j\geqslant 2 \end{cases} \tag{73}$$

$$\mathbf{G}^{kl}_{1,-1}(i,j) = 4^{-1}\mathbf{G}^{kl}_{00}(i,j)(\delta_{i1}-R_l^2)\delta_{j1} \tag{74}$$

Substituting series (64) and (65) in formulae (19) and (20), we get the following series for the vectors $\mathbf{u}^k(s)$ and $\mathbf{v}^k(s)$:

$$\mathbf{u}^k(s) = \sum_{p=0}^{1}\sum_{m=-p}^{M_p}\frac{s^p}{(\ln s)^m}\mathbf{u}^k_{pm} + \mathbf{R}_3(s,M_0,M_1) \tag{75}$$

$$\mathbf{v}^k(s) = \mathbf{v}^k_{00} + s\mathbf{v}^k_{10} + s\ln s\mathbf{v}^k_{1,-1} + \mathrm{O}(s^2\ln^2 s) \tag{76}$$

where the remainder $\mathbf{R}_3(s,M_0,M_1)$ is of the order given by expression (33), and the (N_k+1)-dimensional vectors $\mathbf{u}^k_{pm}$ and the N_k-dimensional vectors $\mathbf{v}^k_{pm}$ are found as

$$\mathbf{u}^k_{00} = \mathbf{c}^k + \mathbf{F}^{kl}_{00}\mathbf{c}^l; \quad \mathbf{v}^k_{00} = \mathbf{d}^k + \mathbf{G}^{kl}_{00}\mathbf{d}^l; \quad \mathbf{v}^k_{1m} = \mathbf{G}^{kl}_{1m}\mathbf{d}^l \tag{77}$$

$$\mathbf{u}^k_{pm} = \mathbf{F}^{kl}_{pm}\mathbf{c}^l \quad (p^2+m^2\neq 0) \tag{78}$$

B.3. Series for the inverse matrices

The matrices $\mathbf{U}^k_{pm}$ and $\mathbf{V}^k_{pm}$, involved in series (37) and (38) for the matrices $\mathbf{U}^k(s)$ and $\mathbf{V}^k(s)$, may be found using Eqs. (19) and (20) and series (64) and (65). For example, the first several coefficients in series (37) and (38) are found as

$$\mathbf{U}^k_{00} = \mathbf{I}_{N_k+1} - \mathbf{F}^{kl}_{00}\mathbf{F}^{lk}_{00}; \quad \mathbf{V}^k_{00} = \mathbf{I}_{N_k} - \mathbf{G}^{kl}_{00}\mathbf{G}^{lk}_{00} \tag{79}$$

$$\mathbf{U}^k_{01} = -\mathbf{F}^{kl}_{00}\mathbf{F}^{lk}_{01} - \mathbf{F}^{kl}_{01}\mathbf{F}^{lk}_{00} \tag{80}$$

$$\mathbf{U}^k_{02} = -\mathbf{F}^{kl}_{00}\mathbf{F}^{lk}_{02} - \mathbf{F}^{kl}_{01}\mathbf{F}^{lk}_{01} - \mathbf{F}^{kl}_{02}\mathbf{F}^{lk}_{00} \tag{81}$$

The matrices $\widetilde{\mathbf{V}}^k_{pm}$, involved in series (35), are found as $\widetilde{\mathbf{V}}^k_{00} = [\mathbf{V}^k(0)]^{-1} = [\mathbf{I}_{N_k} - \mathbf{G}^{kl}_{00}\mathbf{G}^{lk}_{00}]^{-1}$ and $\widetilde{\mathbf{V}}^k_{1m} = -\widetilde{\mathbf{V}}^k_{00}\mathbf{V}^k_{1m}\widetilde{\mathbf{V}}^k_{00}$ $(m=-1,0)$.

The matrices $\widetilde{\mathbf{U}}^k_{pm}$ involved in series (34) are found using the routine described in Section 5.1. The two corresponding simultaneous equations for the matrix $\widetilde{\mathbf{U}}^k_{pm}$ have the following form:

$$\mathbf{U}^k_{00}\widetilde{\mathbf{U}}^k_{pm} = \mathbf{R}^k_{0pm}; \quad [\mathbf{n}^k]^{\mathrm{T}}\mathbf{U}^k_{01}\widetilde{\mathbf{U}}^k_{pm} = [\mathbf{n}^k]^{\mathrm{T}}\mathbf{R}^k_{1pm} \tag{82}$$

where $\mathbf{n}^k$ is the annihilating vector (Section 5.1). The matrices $\mathbf{R}^k_{npm}$ $(n=0,1$ and $p=0,1)$ involved in the right-hand sides of Eqs. (82) are given by

$$\mathbf{R}^k_{n0m} = \delta_{0,m+n}\mathbf{I}_{N_k+1} - \sum_{i=-1}^{m-1}\mathbf{U}^k_{0,m+n-i}\widetilde{\mathbf{U}}^k_{0i} \quad (p=0) \tag{83}$$

$$\mathbf{R}^k_{n1m} = -\sum_{i=-1}^{m+1+n}\mathbf{U}^k_{1,m+n-i}\widetilde{\mathbf{U}}^k_{0i} - \sum_{i=-1}^{m}\mathbf{U}^k_{0,m+n-i+1}\widetilde{\mathbf{U}}^k_{1,i-1} \quad (p=1) \tag{84}$$

Each summation in expressions (83) and (84) is present only when its lower summation limit is not higher than its upper summation limit.

B.4. Series for the transformed temperature $\widehat{T}(x,s)$

$$A_{0m}(x)=\sum_{k=1}^{2}\sum_{p=-1}^{m}\sum_{i=0}^{m-p}[\mathbf{a}_{0i}^{k}(x)]^{\mathrm{T}}\widetilde{\mathbf{U}}_{0p}^{k}\mathbf{u}_{0,m-p-i}^{k},\ m\geqslant 1 \tag{85}$$

$$\begin{aligned}A_{1m}(x)=&(\delta_{0m}+\delta_{-1,m})\sum_{k=1}^{2}([\mathbf{b}_{00}^{k}(x)]^{\mathrm{T}}(\widetilde{\mathbf{V}}_{00}^{k}\mathbf{v}_{1m}^{k}+\widetilde{\mathbf{V}}_{1m}^{k}\mathbf{v}_{00}^{k})\\&+[\mathbf{b}_{1m}^{k}(x)]^{\mathrm{T}}\widetilde{\mathbf{V}}_{00}^{k}\mathbf{v}_{00}^{k})\\&+\sum_{k=1}^{2}\sum_{p=-1}^{m+1}\sum_{i=-1}^{m-p}([\mathbf{a}_{1i}^{k}(x)]^{\mathrm{T}}\widetilde{\mathbf{U}}_{0p}^{k}\mathbf{u}_{0,m-p-i}^{k}\\&+[\mathbf{a}_{0,m-p-i}^{k}(x)]^{\mathrm{T}}\widetilde{\mathbf{U}}_{0p}^{k}\mathbf{u}_{1i}^{k})\\&+\sum_{k=1}^{2}\sum_{p=-2}^{m}\sum_{i=0}^{m-p}[\mathbf{a}_{0i}^{k}(x)]^{\mathrm{T}}\widetilde{\mathbf{U}}_{1p}^{k}\mathbf{u}_{0,m-p-i}^{k},\quad m\geqslant -2\end{aligned} \tag{86}$$

Appendix C. Steady-state solution

The steady-state temperature $T_s(x)$ and the steady-state flux $H_k(\varphi_k)=-[\frac{\partial T_s(x)}{\partial r_k}]_{L_k}$ at the boundary L_k are obtained as

$$\begin{aligned}T_s(x)=\sum_{k=1}^{2}\Big[&\mathbf{m}_{0,-1}^{k}(\mathbf{u}_{01}^{k}+2\ln(r_k/R_k)\mathbf{u}_{00}^{k})\\&+[\mathbf{a}_{00}^{k}(x)]^{\mathrm{T}}\widetilde{\mathbf{U}}_{00}^{k}\mathbf{u}_{00}^{k}+[\mathbf{b}_{00}^{k}(x)]^{\mathrm{T}}\widetilde{\mathbf{V}}_{00}^{k}\mathbf{v}_{00}^{k}\Big]\end{aligned} \tag{87}$$

$$\begin{aligned}H_k(\varphi_k)=-\sum_{p=1}^{2}\Bigg[&\frac{2}{r_p}\frac{\partial r_p}{\partial r_k}\mathbf{m}_{0,-1}^{p}\mathbf{u}_{00}^{p}+\left[\frac{\partial\mathbf{a}_{00}^{p}(x)}{\partial r_k}\right]^{\mathrm{T}}\widetilde{\mathbf{U}}_{00}^{p}\mathbf{u}_{00}^{p}\\&+\left[\frac{\partial\mathbf{b}_{00}^{p}(x)}{\partial r_k}\right]^{\mathrm{T}}\widetilde{\mathbf{V}}_{00}^{p}\mathbf{v}_{00}^{p}\Bigg]_{L_k}\end{aligned} \tag{88}$$

Vectors $\mathbf{u}_{01}^{k}$, $\mathbf{u}_{00}^{k}$, $\mathbf{a}_{00}^{k}(x)$, $\mathbf{b}_{00}^{k}(x)$, $\mathbf{v}_{00}^{k}$ and matrices $\widetilde{\mathbf{U}}_{00}^{k}$, $\widetilde{\mathbf{V}}_{00}^{k}$, involved in Eq. (87), are defined in Appendix B, and the matrix $\mathbf{m}_{0,-1}^{k}$ is defined below. Derivatives, involved in Eq. (88), can be obtained using geometric relations between polar coordinates (r_1,φ_1) and (r_2,φ_2).

Matrix $\mathbf{m}_{0,-1}^{k}$ is $1\times(N_k+1)$-dimensional. It is found as $\mathbf{m}_{0,-1}^{k}=(\mu_k)^{-1}[\mathbf{n}^k]^{\mathrm{T}}$, where $\mathbf{n}^k$ is the annihilating vector (Section 5.1), and the scalar factor μ_k is equal to the first component of the vector $[\mathbf{U}_{01}^{k}]^{\mathrm{T}}\mathbf{n}^k$, that is

$$[\mathbf{U}_{01}^{k}]^{\mathrm{T}}\mathbf{n}^k=\begin{pmatrix}\mu_k\\ \dots\end{pmatrix} \tag{89}$$

Matrix $\mathbf{U}_{01}^{k}$ is defined in Section B.3.

Appendix D. Coefficients of the series in the time domain

The coefficients of series (44) are found as

$$\Lambda_{pm}(x)=\sum_{i=1}^{m-p}(-1)^{i}B_{m-i}^{p,i}A_{pi}(x)\quad(p=0,1;\ m\geqslant p+1) \tag{90}$$

$$\begin{aligned}&\Lambda_{1,-1}(x)=2A_{1,-2}(x);\quad \Lambda_{10}(x)=2\gamma A_{1,-2}(x)-A_{1,-1}(x);\\&\Lambda_{11}(x)=0\end{aligned} \tag{91}$$

where the coefficients $A_{pi}(x)$ are given in Section B.4, and the coefficients $B_{m-i}^{p,i}$ are listed below[2]

$$B_0^{0,i}=1;\quad B_1^{0,i}=-\gamma i;\quad B_1^{1,i}=-i;$$

$$B_2^{0,i}=(\gamma^2-\pi^2/6)\binom{i+1}{2} \tag{92}$$

$$B_2^{1,i}=2\gamma\binom{i+1}{2};$$

$$B_3^{0,i}=(-\gamma^3+\gamma\pi^2/2+\psi^{(2)}(1))\binom{i+2}{3} \tag{93}$$

$$B_4^{0,i}=(-\gamma^2\pi^2+\pi^4/60-4\gamma\psi^{(2)}(1))\binom{i+3}{4} \tag{94}$$

$$\begin{aligned}B_5^{0,i}=\Bigg[&-\gamma^5+\frac{5\gamma^3\pi^2}{3}-\frac{\gamma\pi^4}{12}+\left(10\gamma^2-\frac{5\pi^2}{3}\right)\psi^{(2)}(1)\\&+\psi^{(4)}(1)\Bigg]\binom{i+4}{5}\end{aligned} \tag{95}$$

The notation $\psi^{(n)}(1)$ is used above to denote the polygamma function $\psi^{(n)}(x)$ [21] at $x=1$. The following values of the polygamma function $\psi^{(2)}(1)$ and $\psi^{(4)}(1)$ were computed using the software Mathematica: $\psi^{(2)}(1)=-2.4041138063191886$ and $\psi^{(4)}(1)=-24.8862661234408782$.

References

[1] M. Chung, P.S. Jung, R.H. Rangel, Semi-analytical solution for heat transfer from a buried pipe with convection on the exposed surface, Int. J. Heat Mass Transfer 42 (1999) 3771–3786.
[2] A.M. Starfield, A.L. Bleloch, A new method for the computation of heat and moisture transfer in a partly wet airway, J. South African Instit. Mining Metall. 83 (11/12) (1983) 263–269.
[3] D. Shrivastava, R. Roemer, An analytical study of heat transfer in a finite tissue region with two blood vessels and general Dirichlet boundary conditions, Int. J. Heat Mass Transfer 48 (2005) 4090–4102.
[4] C.Y. Wang, Exact solutions of the unsteady Navier–Stokes equations, Appl. Mech. Rev. 42 (11/2) (1989) S269–S282.
[5] A. Furman, S.P. Neuman, Laplace transform analytic element solution of transient flow in porous media, Adv. Water Resour. 26 (2003) 1229–1237.
[6] H.S. Carslaw, J.C. Jaeger, Conduction of Heat in Solids, second ed., Oxford University Press, London, 1959 (Chapters XII, XIII, XVI).
[7] L. Greengard, P. Lin, Spectral approximation of the free-space heat kernel, Appl. Comput. Harmonic Anal. 9 (2000) 83–97.
[8] C.-H. Wang, M.M. Grigoriev, G.F. Dargush, A fast multi-level convolution boundary element method for transient diffusion problems, Int. J. Numer. Methods Eng. 62 (2005) 1895–1926.
[9] J.S. Loh, I.A. Azid, K.N. Seetharamu, G.A. Quadir, Fast transient thermal analysis of Fourier and non-Fourier heat conduction, Int. J. Heat Mass Transfer 50 (2007) 4400–4408.
[10] C.-K. Chen, T.-M. Chen, J.W. Cleaver, New hybrid Laplace transform/finite element method for two-dimensional transient heat

[2] Formulae for the coefficients $B_{m-i}^{p,i}$ were derived from a more general formula given in [23], where a coefficient $B_s^{\nu,-i}$ corresponds to our $B_s^{\nu,i}$. The numerical values of some of the coefficients $B_s^{\nu,-i}$ are tabulated in [23] as well. We present here the formulae for the particular coefficients $B_{m-i}^{p,i}$ which are more convenient in use.

conduction problem, Numer. Heat Transfer, Part B: Fund. 20 (1991) 191–205.
[11] D. Sheen, I.H. Sloan, V. Thomée, A parallel method for time-discretization of parabolic problems based on contour integral representation and quadrature, Math. Comput. 69 (229) (1999) 177–195.
[12] T. Hohage, F.-J. Sayas, Numerical solution of a heat diffusion problem by boundary element methods using the Laplace transform, Numer. Math. 102 (2005) 67–92.
[13] A.J. Davies, D. Crann, S.J. Kane, C.-H. Lai, A hybrid Laplace transform/finite difference boundary element method for diffusion problems, Comput. Model. Eng. Sci. 18 (2) (2007) 79–85.
[14] L. Godinho, A. Tadeu, N. Simões, Study of transient heat conduction in 2.5D domains using the boundary element method, Eng. Anal. Bound. Elem. 28 (6) (2004) 593–606.
[15] A. Tadeu, J. António, L. Godinho, N. Simões, Boundary element method analyses of transient heat conduction in an unbounded solid layer containing inclusions, Comput. Mech. 34 (2004) 99–110.
[16] O.D.L. Strack, Het analytische element in de groundwatermechanica, Civiele en Bouwkundinge Techniek, Techniek en Wetenschap 1 (2) (1982) 38–43.
[17] O.D.L. Strack, Groundwater Mechanics, Prentice-Hall, Englewood Cliffs, NJ, 1989.
[18] O.D.L. Strack, Theory and applications of the analytic element method, Rev. Geophys. 41 (2) (2003) 1005.
[19] M. Bakker, J.L. Nieber, Analytic element modeling of cylindrical drains and cylindrical inhomogeneities in steady two-dimensional unsaturated flow, Vadose Zone J. 3 (3) (2004) 1038–1049.
[20] R. Barnes, I. Janković, Two-dimensional flow through large numbers of circular inhomogeneities, J. Hydrol. 226 (1999) 204–210.
[21] M. Abramowitz, I.A. Stegun, Handbook of Mathematical Functions with Formulas, Graphs, and Mathematical Tables, National Bureau of Standards, Washington, D.C., 1972 (Chapters 6.4, 9.1, 9.6).
[22] M. Kruskal, Asymptotology, in: A.M. Hamende (Ed.), Plasma Physics: Lectures Presented at the Seminar on Plasma Physics, Organized by and Held at the International Centre for Theoretical Physics, Trieste, from October 5–31 1964, International Atomic Energy Agency, Vienna, 1965, pp. 373–387.
[23] R.H. Ritchie, A.Y. Sakakura, Asymptotic expansions of solutions of the heat conduction equation in internally bounded cylindrical geometry, J. Appl. Phys. 27 (12) (1956) 1453–1459.
[24] W.H. Press et al., Numerical Recipes in Fortran 77: The Art of Scientific Computing, Cambridge University Press, 1992 (Chapter 4).
[25] W.S. Yang, K. Ting, K.T. Chen, Application of an alternating method to the thermoelastic problems with multiple circular holes in an infinite domain, J. Therm. Stresses 27 (7) (2004) 563–585.